Future extreme events in European climate

an exploration of regional climate model projections

Author(s):
Beniston, Martin; Stephenson, David B.; Christensen, Ole B.; Ferro, Christopher A.T.; Frei, Christoph; Goyette, Stéphane; Halsnaes, Kirsten; Holt, Tom; Jylhä, Kirsti; Koffi, Brigitte; Palutikof, Jean; Schöll, Regina; Semmler, Tido; Woth, Katja

Publication date:
2007-05

Permanent link:
https://doi.org/10.3929/ethz-b-000005518

Originally published in:
Climatic Change 81(S1), https://doi.org/10.1007/s10584-006-9226-z

Climatic Change (2007) 81:71–95
DOI 10.1007/s10584-006-9226-z

Future extreme events in European climate: an exploration of regional climate model projections

Martin Beniston · David B. Stephenson · Ole B. Christensen · Christopher A. T. Ferro · Christoph Frei · Stéphane Goyette · Kirsten Halsnaes · Tom Holt · Kirsti Jylhä · Brigitte Koffi · Jean Palutikof · Regina Schöll · Tido Semmler · Katja Woth

Received: 15 February 2005 / Accepted: 17 October 2006 / Published online: 22 March 2007

M. Beniston (✉) · S. Goyette
Climate Research, University of Geneva, Geneva, Switzerland
e-mail: Martin.Beniston@unige.ch

D. B. Stephenson · C. A. T. Ferro
Department of Meteorology, University of Reading, Reading, UK

O. B. Christensen
Danish Meteorological Institute, Copenhagen, Denmark

C. Frei · R. Schöll
Swiss Federal Institute of Technology (ETH), Zurich, Switzerland

K. Halsnaes
Risoe National Laboratory, Roskilde, Denmark

T. Holt · J. Palutikof
Climatic Research Unit, University of East Anglia, Norwich, United Kingdom

K. Jylhä
Finnish Meteorological Institute, Helsinki, Finland

B. Koffi
University of Fribourg, Fribourg, Switzerland

T. Semmler
Met Eireann, Dublin, Ireland

K. Woth
GKSS Research Center, Geesthacht, Germany

Abstract This paper presents an overview of changes in the extreme events that are most likely to affect Europe in forthcoming decades. A variety of diagnostic methods are used to determine how heat waves, heavy precipitation, drought, wind storms, and storm surges change between present (1961–90) and future (2071–2100) climate on the basis of regional climate model simulations produced by the PRUDENCE project. A summary of the main results follows. Heat waves – Regional surface warming causes the frequency, intensity and duration of heat waves to increase over Europe. By the end of the twenty first century, countries in central Europe will experience the same number of hot days as are currently experienced in southern Europe. The intensity of extreme temperatures increases more rapidly than the intensity of more moderate temperatures over the continental interior due to increases in temperature variability. Precipitation – Heavy winter precipitation increases in central and northern Europe and decreases in the south; heavy summer precipitation increases in north-eastern Europe and decreases in the south. Mediterranean droughts start earlier in the year and last longer. Winter storms – Extreme wind speeds increase between 45°N and 55°N, except over and south of the Alps, and become more north-westerly than cuurently. These changes are associated with reductions in mean sea-level pressure, leading to more North Sea storms and a corresponding increase in storm surges along coastal regions of Holland, Germany and Denmark, in particular. These results are found to depend to different degrees on model formulation. While the responses of heat waves are robust to model formulation, the magnitudes of changes in precipitation and wind speed are sensitive to the choice of regional model, and the detailed patterns of these changes are sensitive to the choice of the driving global model. In the case of precipitation, variation between models can exceed both internal variability and variability between different emissions scenarios.

1 Introduction

Climate change is one of the great environmental concerns facing mankind in the twenty first century. Surface temperatures are expected to continue to increase globally and major changes are likely to occur in the global hydrological and energy cycles (IPCC 2001). The greatest threat to humans (and other components of terrestrial ecosystems) will be manifested locally via changes in regional extreme weather and climate events. European society, for example, is particularly vulnerable to changes in the frequency and intensity of extreme events such as heat waves, heavy precipitation, droughts, and wind storms, as seen in recent years.The 2003 heat wave (as discussed inter alia by Beniston 2004 and Schär et al. 2004), the "1999 wind-storm of the century" (Goyette et al. 2003; Ulbrich et al. 2000) and the recurring flood events in many parts of Europe (e.g., Christensen and Christensen 2003; Kundzewicz et al. 1999), are recent examples of extremes that may increasingly become the cause for concern.

Insurance statistics reveal that, after earthquakes, climate-related hazards take the heaviest toll on human life and generate some of the highest claims for insured damage (Fig. 1, adapted from Munich Re 2002). In the second half of the twentieth century, earthquakes caused 71 'billion-dollar events' globally; however, more than 170 such events were related to climatic extremes, in particular wind storms (tropical cyclones and mid-latitude winter storms), floods, droughts and heat-waves. Furthermore, there is evidence that insured losses from extreme climate events have increased in recent decades (Munich Re 2002), due not only to increases in insured infrastructure – more cover, higher premiums (Swiss Re 2003) – but also to recent changes in weather and climate extremes (e.g., more storms in

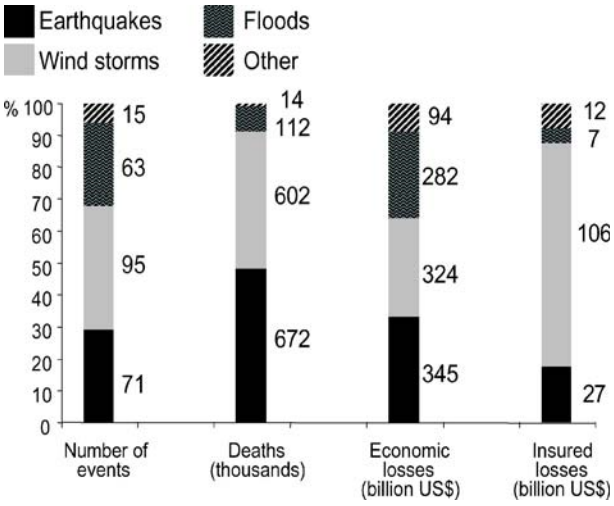

Fig. 1 Relative importance of natural hazards as compiled by the Munich Reinsurance Company (2002), for billion-dollar events since 1950. *Ordinate* indicates the percentage of the total of each category, *figures next to each sub-element of the histograms* refer to the absolute amounts in each category

the 1990s; cf., Harnik and Chang 2003; Chang and Fu 2002; Ulbrich and Christoph 1999; Otterman et al. 2002; Siegismund and Schrum 2001).

This paper presents an overview of changes in various high-risk events that are most likely to affect Europe in forthcoming decades. It aims to highlight some of the key findings from the extremes work undertaken as part of the European Union project PRUDENCE (Christensen et al. 2002; http://prudence.dmi.dk). The PRUDENCE project aims to quantify the uncertainty originating from the choice of global and regional model formulation in climate-change downscaling experiments. Through a unique collaborative effort of nine European regional modeling groups, a coordinated set of climate modeling experiments has been conducted. The resulting large collection of model results that are discussed in other papers of this special issue makes it possible to examine the relative influence of emissions scenario, global model, and regional model on the spread of simulated results.

This paper, on the other hand, specifically addresses a range of climatic extremes, in particular heat waves, heavy precipitation events, droughts, winter storms, and sea surges because of their significant environmental and socio-economic impacts on Europe. A variety of diagnostic methods are applied to determine features of these events in present (1961–90) and future (2071–2100) simulations produced by PRUDENCE and, therefore, how the events are predicted to change by the end of the twenty first century. Section 2 reviews the various methodologies used in this study to define and analyze extremes. Section 3 briefly discusses the RCM model experiments. Section 4 presents the key results for heat waves, precipitation extremes, and wind storms and surges. Section 5 summarizes the main findings.

2 Definition of extreme events and methodology

The following three criteria are often used in climate science to classify events as extreme.

- *Rare* – Events that occur with relatively low frequency/rate. For example, the IPCC (2001) defines an ‘extreme weather event’ to be ‘an event that is rare within its statistical

reference distribution at a particular place. Definitions of "rare" vary, but an extreme weather event would normally be as rare or rarer than the 10th or 90th percentile.'

- *Intense* – Events characterized by relatively small or large values (i.e. events that have large *magnitude* deviations from the norm). Not all intense events are rare: for example, low precipitation totals are often far from the mean precipitation but can still occur quite frequently. Note, intensity as defined here should not be confused with the definition of intensity used in the point process literature to denote the frequency/rate of events.
- *Severe* – Events that result in large socio-economic losses. Severity is a complex criterion because damaging impacts can occur in the absence of a rare or intense climatic event: for example, thawing of mountain permafrost leading to rock falls and mud-slides.

The exploratory analyses presented in Section 4 of this paper are designed to reveal how the simulated climate responds to changes in emissions and model formulation, and therefore focus on meteorological events that are either rare or intense, but not necessarily severe. Table 1 summarizes the extreme events to be considered, and contains three types: maxima, percentiles, and threshold-based indices. Seasonal or annual maxima, such as the summer maximum one-day precipitation totals analyzed in Section 4.2, are simple summaries of extremal behavior. The pth percentile of a data sample is the value below which approximately p% of the data fall. Attention can be focused on different parts of the probability density function (PDF), which summarizes the relative frequencies of the data values, by choosing different percentages p. Indices commonly summarize those data that exceed some threshold, such as the number of days/year on which the temperature at a particular location exceeds 30°C (Section 4.1). This index is based on an absolute threshold but a relative threshold, such as the 90th percentile of the daily maximum temperatures at that location, could be used instead. Adopting a single, absolute threshold for all locations is simple to understand and ensures that indices measure events of a fixed intensity; a single, relative threshold ensures that indices measure events of a fixed rarity. However, because societies across Europe vary in their current levels of adaptation and adaptive

Table 1 The extreme events considered in Section 4

	Maxima	Percentiles	Indices
Temperature		90th and 99th percentile of daily maximum temperature	Number of exceedances of 30°C; number, frequency, duration, and intensity of heat waves (six consecutive exceedances of 90th temperature percentile)
Precipitation	Return levels of maximum summer 1-day and winter 5-day totals; annual maximum dry- and wet-spell lengths	95th percentile of summer 1-day totals	Means of maximum summer 1-day and winter 5-day totals
Wind storms	Annual maximum storm surge	90th and 99th percentiles of winter 10-m wind speed; 10th percentile of winter sea-level pressure	Number of exceedances of 90th, 95th and 99th wind-speed percentiles; number of exceedances of Beaufort thresholds

capacity (i.e. acclimatisation), future changes in absolute values are likely to be more important in some places compared to others.

Such a variety of complementary definitions is required to obtain a broad view of extreme events in the PRUDENCE simulations. A similarly wide range of techniques is required to analyze them and to assess differences between the extreme events in different simulations. The behavior of maxima can be summarized during a particular period by sample statistics such as the mean (Sections 4.2.4, 4.3.4) and these support straightforward comparisons. Probability models, such as the generalized extreme-value distribution motivated from extreme-value theory (e.g. Kharin and Zwiers 2000; Coles 2001), can also be fitted to maxima to obtain a more complete description of their statistical properties within a particular simulation (Sections 4.2.1, 4.2.2, e). Percentiles with low or high values of p are useful for summarizing the tails of probability distributions and can easily be compared (Sections 4.1, 4.2.3, 4.3.1, 4.3.3). Changes in percentiles can be related to changes in the location (e.g. mean) and scale (e.g. variance) of the distribution (Mearns et al. 1984; Katz and Brown 1992; Ferro et al. 2005). Annual indices can also be summarized by sample statistics (Sections 4.1, 4.2.1) and by fitting probability models (Section 4.2.1).

The severity of the events considered in this paper, and other events with critical impacts, is the subject of ongoing research in PRUDENCE. Determining severity is a cross-disciplinary problem because an event's impact on a system depends on the system's state. The economic impact of an extreme event on corn production, for example, depends not only on temperature and precipitation, but also on irrigation, market prices, land prices, productions costs, agricultural policies such as subsidies, mitigation strategies, and available compensation. Once the roles of these different factors are understood, adaptations can be planned to counteract climate change predicted by models. Both the individual effects and the interactions of different factors can be crucial, with climatic thresholds or non-linear combinations potentially triggering severe impacts. Temporal and spatial patterns of events are also important. Table 2 lists some of the impacts related to the European climatic extremes discussed in this paper. Careful analysis is required to model the complex relationships between climate and these impacts on health, agriculture, forestry, infrastructure, and ecosystems.

Table 2 Typical impacts associated with extreme events

	Health	Agriculture	Forestry	Buildings and infrastructure	Ecosystems
Heat waves	Excess illness and mortality	Animal stress, crop damage	Impaired growth, pests	Increased cooling energy demand	Wildlife stress
Precipitation	Floods, poor water quality and adequacy	Crop failure by drought or excess water	Water stress	Floods, landslides, ground shrinkage, property loss	Soil erosion, water stress
Wind storms	Accidents	Crop damage	Timber loss, insect damage	Building damage	Reduced biodiversity
Wind surges	Floods	Floods and erosion	Floods and erosion	Floods and erosion	Floods and erosion
Adverse combinations	Temperature and moisture	Temperature, precipitation, and wind	Temperature, precipitation, and wind	Wind and floods	Unseasonable temperature, precipitation

There is a clear incentive for the research community and the public and private sectors alike to focus on the future course of extreme climatic events under the changing climatic conditions expected during the twenty first century. A better understanding of the factors involved will improve the quantification of costs associated with climate-related hazards and thereby provide the basis for strategies to adapt to climate change.

3 Data sets used: the RCM simulations

This section gives a brief overview of the PRUDENCE model data used in this paper. More details of the design of the model experiments are given in Jacob et al. (2007; this issue). PRUDENCE has created a total of 55, 30-year integrations employing nine regional climate models (RCMs) and one stretched global atmospheric model. The PRUDENCE experiments include control simulations of contemporary (1961–90) climate and scenario simulations of future (2071–2100) climate. Lateral boundary conditions for the RCMs are supplied by one of two high-resolution, global atmospheric general circulation models (GCMs). Observed monthly fields of sea-surface temperature (SST) and sea-ice extent (SICE) provide boundary conditions for the GCMs in the control period. Boundary conditions for the GCMs in the scenario period are constructed by adding to the observed fields anomalies (the differences between 2071–2100 and 1961–90) from integrations of the coupled atmosphere-ocean global model HadCM3 (Jones et al. 2001; Johns et al. 2003) forced with the A2 (high emissions) and B2 (lower emissions) 'families' of scenarios developed by the IPCC (Nakicenovic et al. 2000). Monthly varying aerosol concentration fields are also provided to the RCM simulations. The output from all RCMs has been investigated but results are presented here for only the following models due to space limitations.

- HIRHAM model of the Danish Meteorological Institute (Christensen et al. 1998),
- HadRM3H/P model of the Hadley Centre (Johns et al. 2003),
- RCAO model of the Swedish Meteorological and Hydrological Institute (Räisänen et al. 2004),
- REMO model of the Max-Planck-Institute of Meteorology (Jacob 2001),
- CHRM model of the Swiss Federal Institute of Technology (ETH) (Lüthi et al. 1996).
- CLM model of the Institute for Coastal Research (GKSS; Steppler et al. 2003).
- RACMO2 model of the Royal Netherlands Meteorological Institute (KNMI; Lenderink et al. 2003).
- Suffices-E and-H will denote RCMs driven by the HadAM3H and ECHAM4/OPYC3 GCMs, respectively; additional suffices /C,/A2 and /B2 will denote GCMs forced by control, A2 and B2 scenario emissions.

The two GCMs designated to provide boundary conditions for the PRUDENCE RCM experiments are the UK Hadley Centre HadAM3H model (Pope et al. 2000) at $1.875 \times 1.25°$ resolution in longitude and latitude, and the German Max-Planck-Institute ECHAM5 model (Roeckner et al. 2003). Only experiments with HadAM3H boundaries have been performed in time for inclusion in this work.

It should be stressed here that not all analyses in the following have included the full set of available simulations. This paper is an overview of several studies of varying degrees of complexity, performed at several institutions in the PRUDENCE project. Hence, this paper should not be seen to be an exhaustive analysis of all relevant aspects of all models available.

4 Results

4.1 Heat waves

The heat wave that strongly affected much of Europe in the first 2 weeks of August 2003 (Beniston 2004; Schär et al. 2004) led to thousands of excess deaths in France, Italy and Spain (Fischer et al. 2004; Stedman 2004). This highlighted problems that could afflict environmental systems such as hydrology and vegetation, socio-economic systems such as agriculture and energy supply, and human mortality and morbidity if such events were to increase in frequency, intensity, and persistence.

The incidence of summer heat waves increased during the course of the twentieth century (IPCC 2001; Frich et al. 2002 at the global scale; Schär et al. 2004; Beniston and Stephenson 2004, and McGregor et al. 2005 for Europe). Modeling studies (e.g. Zwiers and Kharin 1998; Huth et al. 2000; Kharin and Zwiers 2000; Meehl et al. 2000), most of which were based on GCM simulations, concluded that this trend is likely to continue through the twenty first century. However, IPCC (2001) exercised caution over these conclusions, pointing to the lack of adequate data and analyses, and the need to improve both the accuracy and regional detail of model projections. Moreover, the wider literature mentions little about anomalously warm episodes outside the summer season. For instance, relatively mild periods during winter can adversely affect the environment and the economy by causing floods and poor skiing conditions, and by disrupting crop production (Beniston and Jungo 2002; Beniston 2003; Shabbar and Bonsal 2003). This section investigates the changes in frequency, intensity and duration of summer heat waves and other unseasonably warm spells between the PRUDENCE control and A2 scenario simulations.

Several measures of extreme temperatures are used: the frequency with which daily maximum temperature exceeds 30°C, high temperature percentiles, and four heat-wave indices. A heat-wave is defined to be a spell of at least six consecutive days with maximum temperature exceeding the 1961–90 calendar day 90th percentile, calculated for each day over a centred 5-day window at each grid point (e.g., Robinson 2001). While heat waves of shorter duration can already lead to environmental and socio-economic impacts, this longer duration was chosen in view of the expected increase in the number of long heat waves in a future, warmer, climate. The four indices, calculated for each year, are:

- Heat Wave Number (HWN) – The number of heat waves that occur in a given time interval (e.g., per decade)
- Heat Wave Frequency (HWF) – The total duration (in days) of all the heat waves that occur in a given time interval,
- Heat Wave Duration (HWD) – The longest duration of a heat wave, measured in days, of all the heat waves occurring in a given time interval;
- Heat Wave Intensity (HWI) – The greatest exceedance of a given threshold of temperature, expressed in degree-days, for all the heat waves occurring in a given time interval.

The ability of HIRHAM-H to reproduce current climate (i.e., the 1961–1990 reference period) has been demonstrated in earlier work, such as reported in a fundamental paper on the model by Christensen et al. (1998), or for a particular loacel by Beniston (2004) in the context of the 2003 European heat wave.

Figure 2 shows the mean number of days/year above 30°C simulated by HIRHAM-H/C and HIRHAM-H/A2. The summer climatic zones shift northward by at least 400–500 km

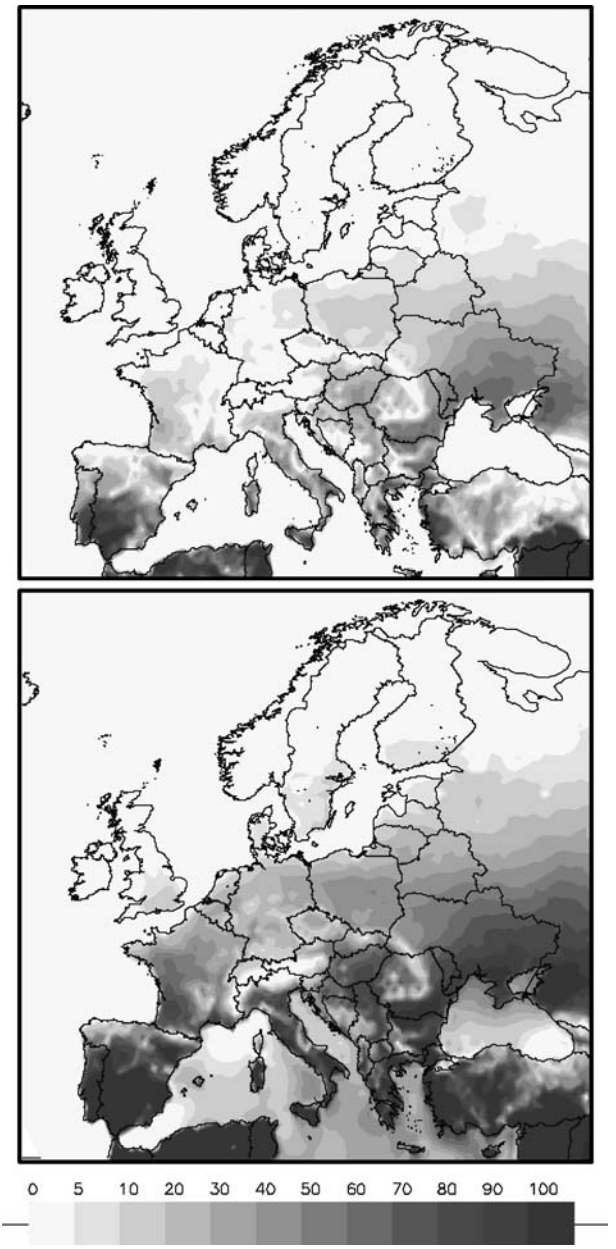

Fig. 2 Mean annual number of days above 30°C simulated by the HIRHAM4 regional climate model for the 1961–1990 (*upper*) and 2071–2100 (*lower*) periods

by the end of the twenty first century. Regions such as France and Hungary, for example, may experience as many days/year above 30°C in the future as are currently experienced in Spain and Sicily. The mean number of days/year exceeding 30°C at the model grid point nearest to Paris increases from 9 days under current climate (observations at the Paris-Montsouris station give 6 days) to 50 days under future climatic conditions; whereas heat

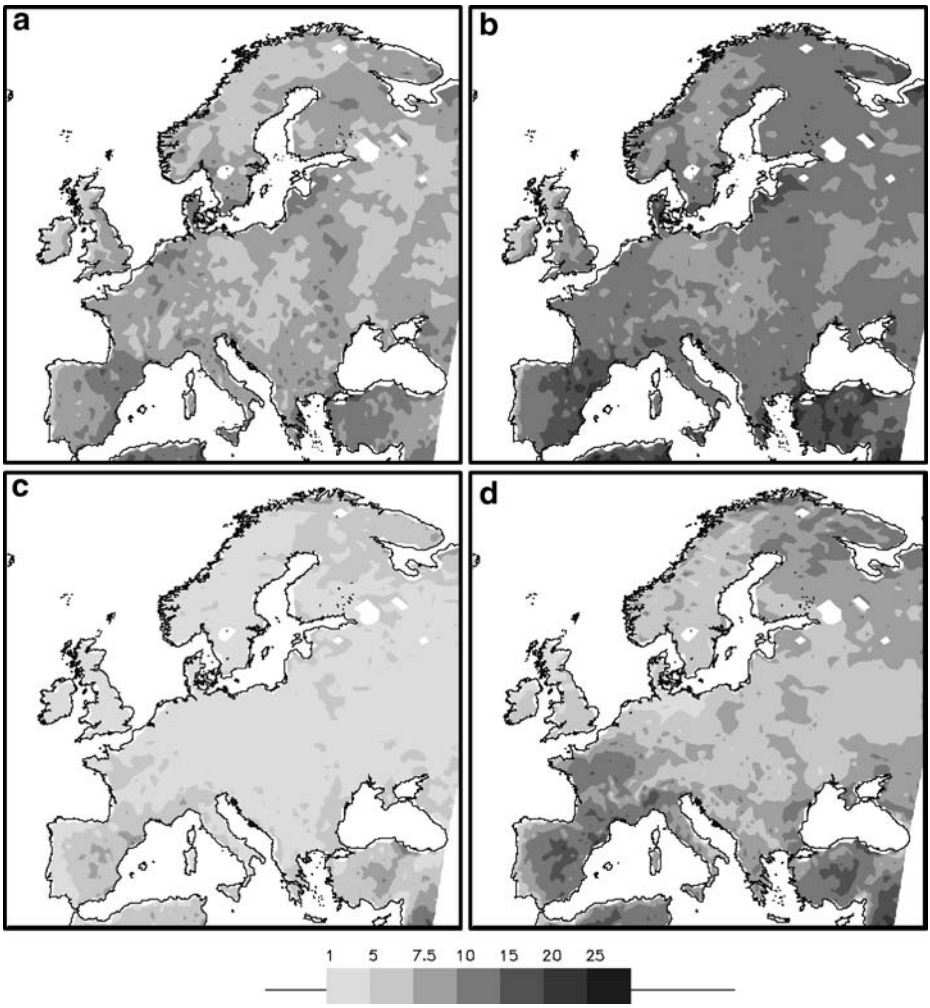

Fig. 3 Changes (*expressed as a ratio*) in the heat wave indices N_HW (**a**), HW_F (**b**), HW_D (**c**) and HW_I (**d**) between the 1961–1990 and 2071–2100 periods, based on HIRHAM4 simulations. (See text for details and definitions of these indices)

waves in Paris are restricted to summer (JJA) during the control period, 10% of the heat wave days occur outside summer in the scenario simulation; the maximum number of consecutive days/year exceeding 30°C at Paris increases from an average of 3.5 days (3.0 for observations at Paris-Montsouris) to 18.9 days.

Figure 3 shows the changes in the four heat wave indices simulated by HIRHAM-H, expressed as ratios. The mean duration (HWD, Fig. 3a) increases by a factor of between one and eight over most of Europe. Much higher increases of at least a factor of seven are predicted for the mean intensity (HWI, Fig. 3b), the mean number of heat waves (HWN, Fig. 3c) and the frequency of heat-wave days (HWF, Fig. 3d), with greatest changes (more than tenfold increases) in the south of France and Spain.

4.2 Extreme precipitation

This section presents results for several diagnostics of heavy precipitation in RCM output and discusses the simulated change in heavy precipitation between contemporary and future climates.

4.2.1 Validation of RCM simulation of extreme precipitation

This sub-section investigates the ability of RCMs to reproduce extreme precipitation events under current climatic conditions by means of a case study for southern Germany, where a dense long-term network of observation stations is available from the German Weather Service. Simulated data from REMO-H/C (Jacob 2001) are compared to the observations interpolated to the model grid. The generalized extreme-value (GEV) distribution has been fitted to summer maximum 1-day and winter maximum 5-day precipitation totals at each grid point. These 1- and 5-day aggregations account for the different character and impact of extreme precipitation in the two seasons – European winter flooding is generally due to persistent large-scale precipitation whereas summer flooding is more often due to rapid localized convective activity. Results from Baden-Wuerttemberg and Bavaria in Germany suggest that the 5-year return levels of daily precipitation in summer are adequately represented in the model with lower values in the relatively flat north and higher values in the alpine region to the south. However, the spatial variability is underestimated in REMO-H/C, thereby leading to an overestimation of 30% in the north and an underestimation of 30% in the south. This may be related to underestimated topographic differences in mountainous regions, where a horizontal resolution of 55 km is insufficient to resolve strong altitudinal gradients. The 5-year return levels of 5-day winter precipitation are generally higher in the mountainous south than in the north, both in the observations and in REMO-H/C. The observations exhibit return levels above 80 mm in the east of Bavaria, whereas REMO-H/C has lower values of around 60 mm in the same region. Differences between simulated and observed return levels are generally less than 30% for the region considered.

4.2.2 Extreme value modelling of changes in extreme precipitation

Four RCMs have been selected for this particular analysis: CHRM-H, HadRM3P-H, HadRM3H-H, and HIRHAM-H. Three ensemble members are available for each model in each period (1961–90 and 2071–2100) except for CHRM-H, which has only one member.

The GEV distribution is again fitted by maximum likelihood to summer maximum 1-day and winter maximum 5-day mean precipitation, this time at each grid point, separately for both the control and A2 scenario integrations using a geophysical prior distribution for the shape parameter (see Frei et al. 2005 for details). The statistical significance of the change is assessed for each grid-point individually using parametric resampling similar to Kharin and Zwiers (2000). Figure 4 displays the changes in 5-year return levels between the HIRHAM-H/C and HIRHAM-H/A2 time-slices in winter (Fig. 4a) and summer (Fig. 4b). The 5-year level is chosen, as opposed to more rare events, to avoid excessive noise in the climate-change signals (see also Frei and Schär 2001; Frei 2003).

In winter there is an increase in the return level north of about 45°N and a decrease to the south, which is similar to the pattern of change for mean precipitation (e.g. Jones et al. 2001; Räisänen et al. 2004) at least on large scales. Over much of north-western Europe, Scandinavia and eastern Europe, the 5-year return level estimated from the scenario is at least as large as the 15-year return level of the control experiment, which implies a more

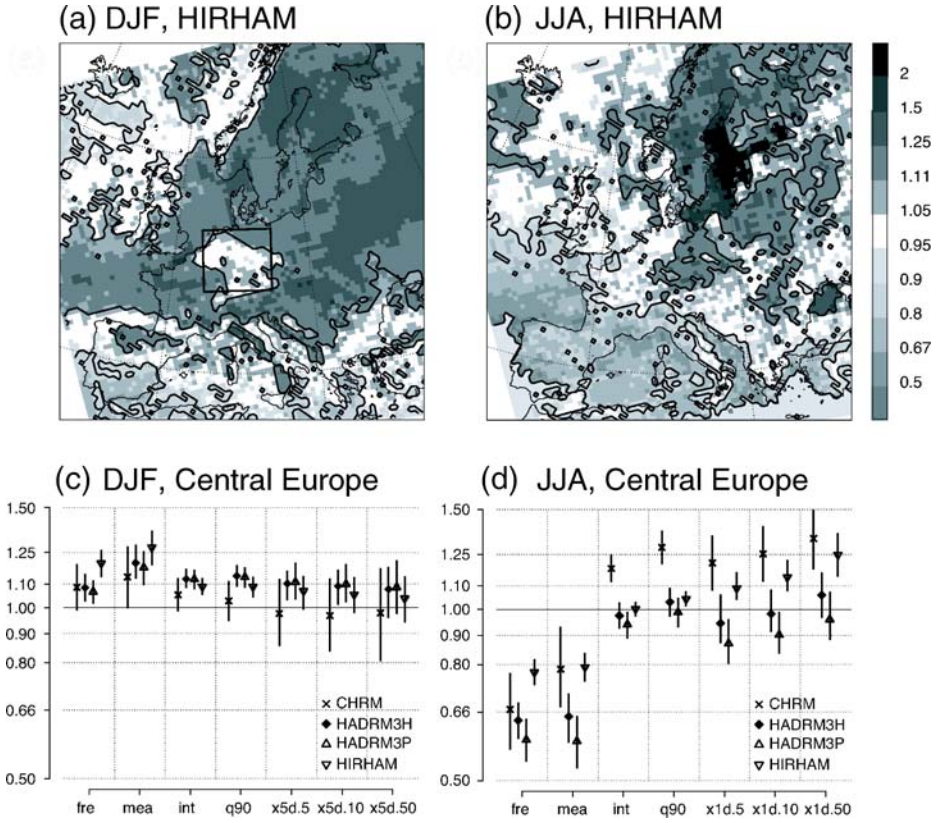

Fig. 4 Panels (**a**) and (**b**): Change in the 5-year return level of 5-day precipitation in winter (*left*) and 1-day precipitation in summer (*right*), as simulated by the HIRHAM regional climate model. The change is given in terms of the ratio of return levels between the scenario and control time slices and the statistical significance (p value=5%) of the change (as determined by parametric resampling) is displayed as a bold black line. Panels (**c**) and (**d**): Relative change in several statistics of daily precipitation in Central Europe (domain see panel (**a**)) as simulated by four RCMs (see legend). *fre*: Frequency of wet days (daily amount larger than 1 mm), *me*: mean seasonal precipitation, *int*: precipitation intensity (average amount on wet days), *q90*: 90% quantile of wet days, *xjd.n*: *n*-year return value of *j*-day precipitation extreme. *Vertical bars* represent the 95% confidence interval of the estimated change

than threefold increase in frequency. In winter, results from the other models are very similar both in spatial distribution and magnitude (Frei et al. 2005). This is also evident from Fig. 4c, which shows for all RCMs the domain mean response of a number of precipitation statistics, including the return levels of extremes. The similarity of results implies that in winter the simulated change of precipitation extremes is relatively insensitive to the different physical parameterization schemes used in these RCMs. The differences for CHRM-H are primarily due to the fact that only a single ensemble member was used.

In summer, the extreme value analysis diagnoses a statistically significant decrease (at the 5% level) in the 5-year return level for HIRHAM-H over many southern parts of the continent and an increase over Scandinavia and north-eastern Europe (Fig. 4b). An interesting regional variation is found over parts of central and eastern Europe where the return level increases despite the pronounced decrease in mean precipitation in these

regions reported by Christensen JH and Christensen OB (2003). Although the large-scale pattern of change is similar for all models in summer, the quantitative change in the precipitation distribution varies considerably (Fig. 4d). Over central Europe, there is a prominent decrease of precipitation frequency in HadRM3H-H and HadRM3P-H, while precipitation intensity and heavy precipitation percentiles show little change. In contrast, for CHRM-H and HIRHAM-H the decrease in frequency is partly compensated for by an increase in precipitation intensity and the frequency of heavy events as shown by the return levels. Similar model sensitivities were found for the Mediterranean area. In contrast to winter precipitation extremes, these results imply that the magnitude of the change in summer heavy precipitation events critically depends on the RCM formulation (Frei et al. 2005).

4.2.3 Sensitivity of results to future emission scenarios

It was seen above that large-scale patterns of projected changes in heavy precipitation are robust to RCM but not to GCM, but that magnitudes of changes vary with RCM, particularly in summer. An additional source of uncertainty is the future emission of greenhouse-gases and aerosols. This sub-section discusses the sensitivity of the projected changes to emissions by analyzing responses to two different scenarios (A2 and B2).

The 30-year means of the winter and summer maximum 1- and 5-day precipitation totals (designated as R1d and R5d, respectively) for the periods 1961–90 and 2071–2100 were derived from the daily output of seven RCMs: HIRHAM, RCAO, HadRM3P/H, CHRM, REMO, RACMO2 and CLM. Four pairs of experiments include both the A2 and B2 runs, two of which were driven by the HadAM3H or HadAM3P boundary forcing and two by the ECHAM4/OPYC3 forcing. After interpolating onto a common $0.5° \times 0.5°$ grid, the seasonal means were averaged over 20 sub-domains of Europe. Then the differences between the present-day and future averages were computed to represent the RCM-simulated changes in the two indices of heavy precipitation. Variation among ensemble members (available for HIRHAM-H/A2 and HadRM3P-HP/A2) provides a rough guide to simulated natural variability.

The mean winter maximum 5-day precipitation total increases in every model bar one for the Central Europe domain (Fig. 5a). The projected increases are slightly lower than the simulated changes in mean winter precipitation and the mean winter 1-day maximum (not shown). The changes in R5d predicted under the B2 scenario are smaller than those predicted under the A2 scenario in two cases, and similar in the two other cases. The range of simulated increases in the experiments driven by the HadAM3H/A2 forcing is about 10%, reflecting the uncertainty arising from differences in RCM formulation and the internal variability of climate. The variation due to divergent GCM providing the boundary conditions is at least as large.

Elsewhere in Europe, the simulated responses in wintertime R5d generally resemble those found for Central Europe. Over the Mediterranean land areas, however, R5d decreases as well as mean precipitation in some model experiments. Over northern Europe, the simulated increases in winter mean R5d are generally smaller for the B2 than for the A2 scenario. In many other regions the uncertainty in changes in R5d due to natural variability is at least as large as the variation between emission scenarios.

While the summertime mean precipitation over Central Europe decreases in all RCM experiments, the mean summer maximum 1-day precipitation total is generally projected to either increase or remain virtually unaltered (Fig. 5b). However, simulations with a very large reduction in the summer mean precipitation show decreases in R1d as well, yet the

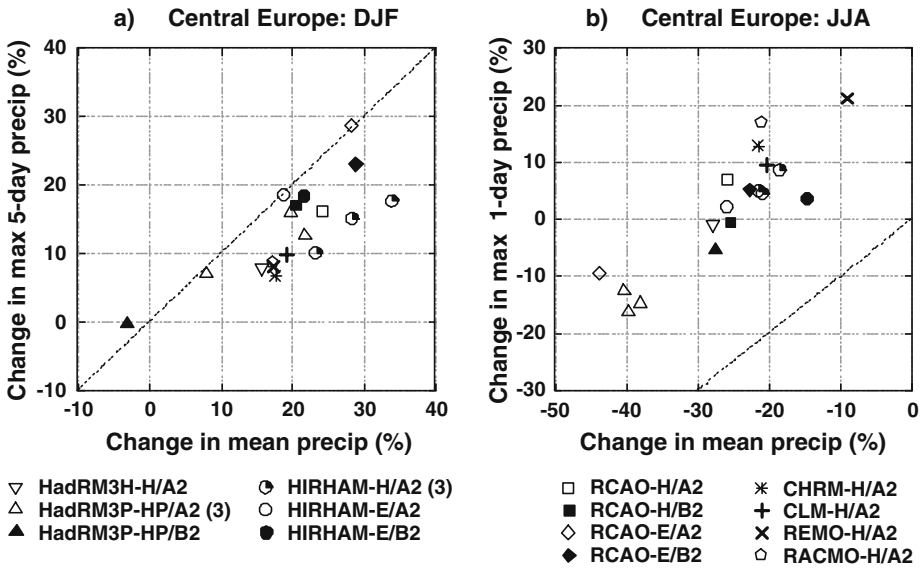

Fig. 5 Projected area-averaged changes (%) in the 30-year means of the greatest **a** 5-day precipitation total in winter and **b** 1-day precipitation total in summer in Central Europe (land areas in 47.0–54.0°N, 5.0–20.5°E), relative to the baseline period 1961–1990. Both variables are given as a function of the seasonal mean precipitation changes. *The legend* indicates the regional climate models, GCM forcing (*H* referring to HadAM3H, *HP* to HadAM3P, *E* to ECHAM4/OPYC), the SRES emissions scenario (A2 or B2), and the number (*in parentheses*) of ensemble simulations

decreases in R1d are smaller than those in the mean precipitation. A comparison between the A2 and B2 scenarios indicates that smaller emissions yield weaker changes over Central Europe. The differences due to the emissions scenario appear to be at least of the same magnitude as those due to natural variability. The largest uncertainty, however, arises from differences in model formulation.

In sub-domains over southern Europe, the projected changes in summer mean R1d range from −60 to +10% (not shown). In most cases the reduction is smaller for the B2 than for the A2 scenario. In northern Europe, on the other hand, there are no clear systematic differences between projected increases for the two emissions scenarios (not shown). The projected changes in R1d are almost invariably positive, up to about 40%, and are strongly model-dependent. For the summer mean precipitation in northern Europe, there is a qualitative inter-model disagreement, some experiments showing a decrease and others either an increase or negligible change.

Over most sub-domains, the projected percentage changes in the two indices of heavy precipitation are closely correlated with changes in mean precipitation, even more so in summer than in winter. To a first degree of approximation, the projected percentage changes in the summer mean R1d may be approximated by adding a factor of about 20–35% to the corresponding changes in mean precipitation. The factor for the summer mean R5d (not shown) is smaller but nonetheless positive, revealing the fact that the intensity of individual precipitation events increases more (in northern Europe) or decreases less (in southern Europe) than the total number of wet days. In winter, the tendency to smaller increases in R5d than in mean precipitation might be explained by comparable increases in the number of wet days and the average precipitation intensity (see Fig. 5c).

The ranges in the projected changes in the two indices of heavy precipitation illustrate the uncertainties due to differences in the RCM formulation, the emissions scenarios and the GCM boundary conditions. However, these factors do not represent the full range of uncertainty discussed by the IPCC (2001). In that report, a wider range of radiative forcing and a larger set of GCMs (but not RCMs) were considered than in PRUDENCE. Assuming, as hinted by Fig. 5, that changes in heavy precipitation are associated with changes in mean precipitation, it is pertinent to examine how the latter is projected to alter on the basis of a larger set of GCMs. In addition to HadCM3 and ECHAM4/OPYC3, the set considered by the IPCC included the CCSR/NIES, CGCM2, CSIRO Mk2, GFDL R30 and NCAR DOE PCM models (IPCC 2001). It appears that about half of the experiments applying the A2 forcing and almost all simulations applying the B2 forcing produced smaller decreases in the summer mean precipitation over Central Europe than the RCM simulations considered here. This suggests that the range of uncertainty in the change of summertime heavy precipitation is not fully captured by analyzing the present RCM output. For the winter mean precipitation total, there were no major differences between the PRUDENCE RCM and IPCC GCM projected changes.

4.2.4 Risk of Mediterranean drought

This sub-section summarizes the changes in Mediterranean drought conditions predicted by three RCMs: HadRM3P, HIRHAM, and RCAO forced with both HadAM3H and ECHAM4/OPYC3. Here a drought is defined as a continuous period of days with no precipitation, parameterized by indices of the maximum length of drought in a year, and the start and end dates of the maximum drought. To examine rainfall changes, indices of the annual maximum length of wet spell and the annual maximum 3-day running rainfall total, are used. The indices indicate considerable drying over much of the Mediterranean under the A2 scenario. The main features are reduced intensity precipitation, and earlier onset and longer duration of drought. The regions most affected are the southern Iberian peninsula,

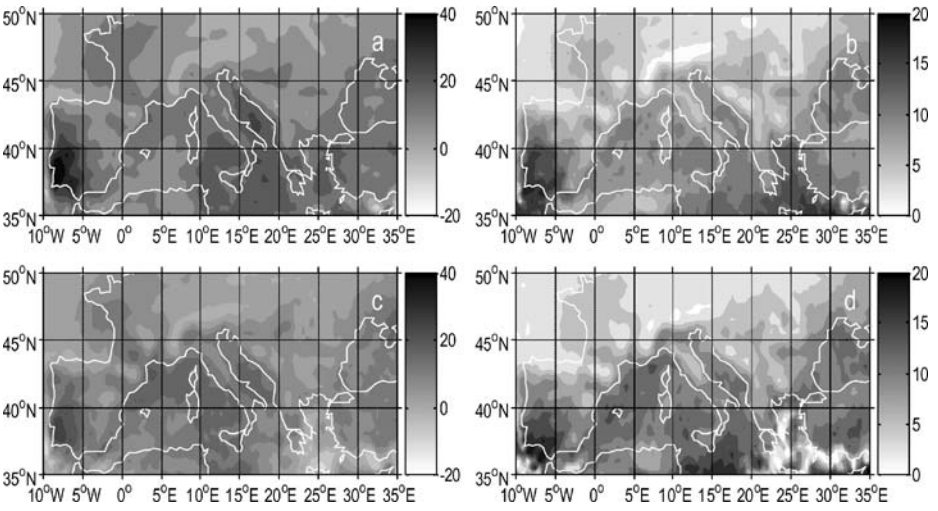

Fig. 6 (**a**) A2a: Maximum dry spells (days); (**b**) A2a confidence range (days); (**c**) B2a: Maximum dry spells (days); (**d**) B2a confidence range (days)

the Alps, the eastern Adriatic seaboard, and southern Greece. Although the impacts are considerably reduced in the B2 scenario, which produces increased precipitation in some areas, the overall pattern is still one of a drier Mediterranean.

The changes simulated by the different RCMs are sufficiently similar that multi-model averages, with reduced variability, are meaningful. Figure 6 maps the average change for one index: the annual maximum length of dry spell (summer drought). The difference between the index, averaged over time and models, in the control period and in each of the A2 and B2 scenarios is calculated and uncertainty is re the width of bootstrapped 95% confidence intervals. Under the A2 scenario (Fig. 6a), drought over southern Iberia lasts over a month longer than at present, with a 95% confidence interval of about ±9 days (Fig. 6b). Under the B2 scenario (Fig. 6c), the length of drought over southern Iberia increases by about 20 days with roughly the same uncertainty (Fig. 6d) as for the A2 scenario.

Changes in return levels of annual maximum length of wet spell are estimated by fitting the GEV distribution to annual maxima from the control and scenario simulations. Figure 7 maps the changes in 100-year return level and reveals a general reduction of about 15 to 20 days (or 40%) under the A2 scenario but by only 5 to 10 days (or 20%) under the B2 scenario. Changing the driving GCM, as seen in Fig. 7c and e for RCAO-H and RCAO-E, respectively, is more influential than changing the emissions scenario. This finding is consistent across all analyses of precipitation extremes for the Mediterranean, but cannot be considered further since there are only two driving GCMs for one RCM. Future analyses of RCM data must incorporate more than one driving GCM for a range of RCMs, and assess the influence of this on the overall uncertainty in the model projections.

4.3 Extreme wind storms and storm surges

4.3.1 Wind storms

North Atlantic extra-tropical cyclones can often lead to high surface wind speeds in Europe, especially over the sea or in coastal and mountainous regions. Rapidly developing cyclones can produce anomalously severe weather, high winds and storm surges that severely damage the natural environment and many socio-economic sectors (IPCC 2001). It is therefore important to assess future storminess by investigating extremes in variables such as daily mean sea-level pressure, p_{msl}, 10 m daily maximum wind speed, $v_{10,max}$, and 10 m wind direction, $v_{10,dir}$. The mean and the tails of the PDFs of p_{msl}, $v_{10,max}$, and $v_{10,dir}$ fields are investigated here in the control simulation and for the IPCC A2 scenario from the HIRHAM-H, CHRM-H and RCAO-H models. We have focused on winter (DJF) when such storm activity is at a maximum, although storminess in other seasons can also lead to large impacts (e.g. the October 1987 storm that caused much damage in the south of England).

Prior to analyzing these changes, the simulated winter mean sea-level pressure and the 10-m wind velocity fields were compared, in a qualitative manner, to the NCEP/NCAR reanalysis mean sea-level pressure and 1000-hPa wind speed and direction, respectively. This comparison indicated that the RCMs realistically reproduced the large-scale features of these quantities during the 1961–90 period. The mean sea-level pressure has a strong north–south gradient, from roughly 995 hPa south of Iceland to more than 1,015 hPa in central Europe. Between these low- and high-pressure systems, the isobars are almost parallel and are tilted in a SW–NE direction. The mean DJF wind velocity vector field has a marked but smooth east–west gradient with stronger winds over the ocean. The mean wind speed ranges from 4 m/s inland to over 13 m/s over the central North Atlantic Ocean. The

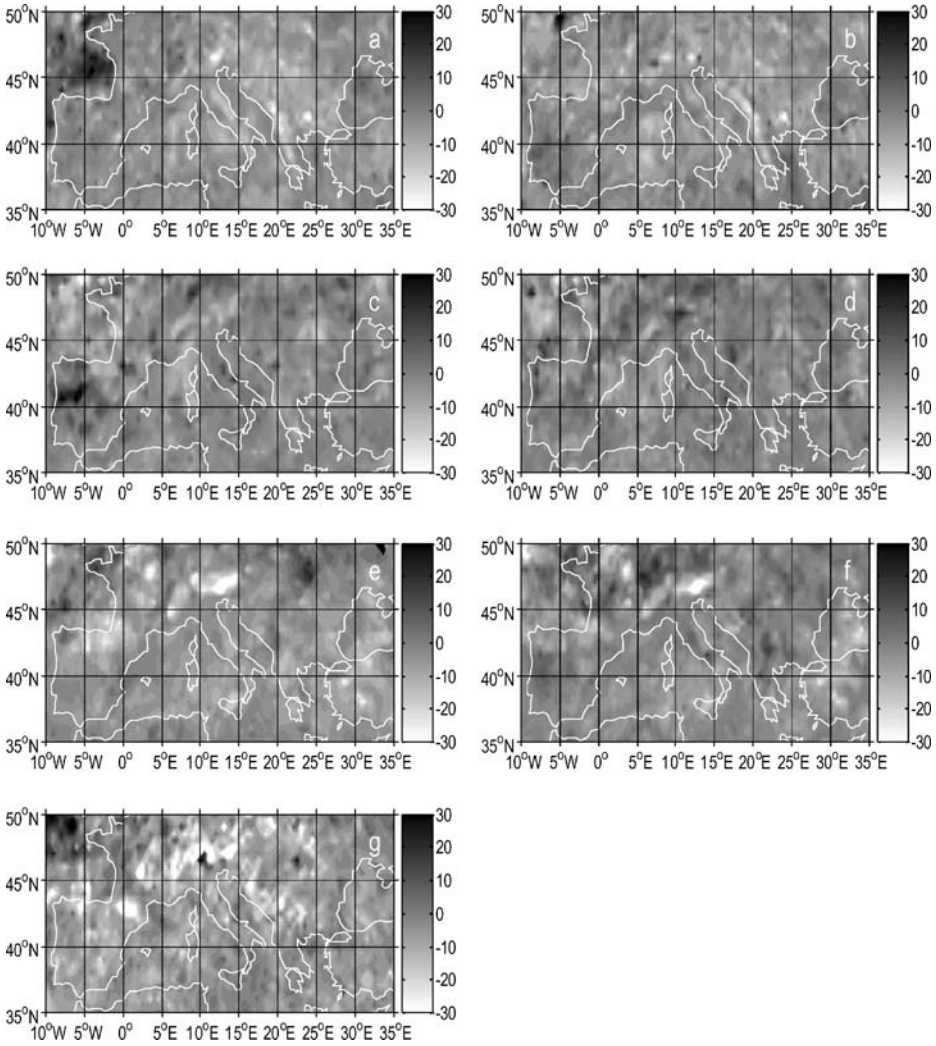

Fig. 7 100-year return levels of maximum length of wet spells for the following models: (**a**) HadRM3P A2a; (**b**) HadRM3P B2a; (**c**) SMHI-HC A2a; (**d**) SMHI-HC B2a; (**e**) SMHI-MPI A2a; (**f**) SMHI-MPI B2a; (**g**) DMI A2a

simulated 90th percentiles of wind speed exceed 20 m/s over the ocean, and are between 4 and 6 m/s over land but with a sharper east–west gradient component at the ocean–land transition region.

Zwiers and Kharin (1998) found evidence for increased extreme wind speeds related to a negative pressure anomaly over northern Europe in a doubled CO2 integration of a Canadian GCM. RCM results give similar large-scale conclusions but also reveal more detail. The 90th percentile of daily DJF wind speeds show a 2.5% to more than 10% increase in a European latitude band extending roughly from 45–55°N, and the changes generally decrease to small or even negative values on either side of this band as shown in Fig. 8 for RCAO-H. The positive changes are concentrated over the ocean, the North Sea, and western Europe (UK, France, northern Switzerland, Germany). Generally, over the

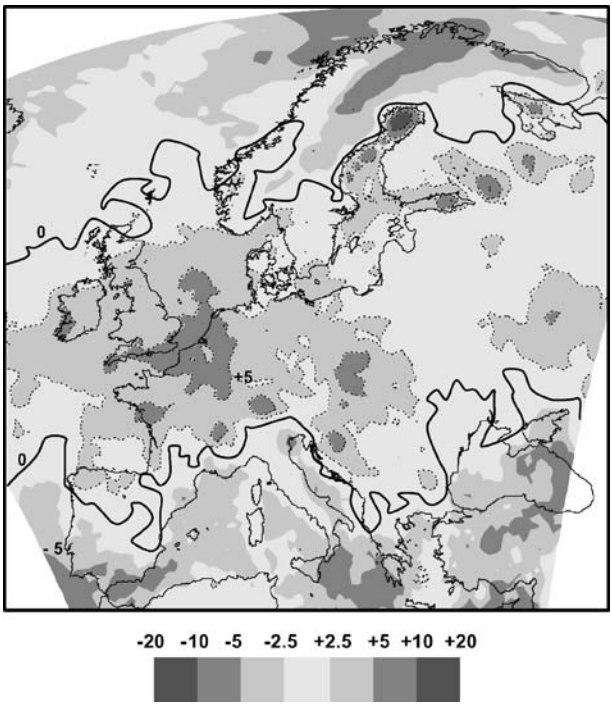

Fig. 8 Simulation by the RCAO regional climate model of the change (%) in the 90th percentile of winter (DJF) daily maximum wind speed in Europe, between the 1961–1990 and the 2071–2100 periods. Positive change is drawn in *dotted line*

continent, there is no obvious relationship between these changes and orography (apart from the Alps) where there seems to be a systematic positive change to the north and a negative change over and south of the Alps. Over Croatia, similar but less intense changes occur with the Dinaric Alps and the Dalmatian Coast to the west. Similar conclusions hold for changes in the mean value of wind velocity in each RCM. The 10th percentile of daily DJF sea-level pressure generally shows a 2–3 hPa decrease over the UK, the North Sea, the Norwegian Sea and the Baltic, extending inland to France, Germany, and Scandinavia. Negative anomalies of up to 5 hPa are seen in the mean DJF sea-level pressure (Fig. 9) as well as in the 90th percentile fields under the A2 scenario. This surface pressure anomaly is also seen in the driving GCM (HadAM3H). This corresponds well to the negative pressure anomaly diagnosed in the Canadian GCM experiments, which intensifies the zonal circulation over Europe and brings more storms into this area following the North Atlantic storm tracks.

The Alpine mountain chain appears to be a locus of important changes in the behavior of the wind speeds and directions between current and future climates. The 10 m wind speeds of the 21 HIRHAM-H model grid-points covering Switzerland have been analyzed in more detail for the two 30-year time-slices. The numbers of wind speed events per year exceeding the control period 95th and 99th percentiles and falling below the 25th percentile all increase by 10%. The most substantial increases occur in winter, when there is a three-fold increase in the number of events exceeding the 99th percentile north of the Alps, but also a notable reduction over and south of the mountains. In summer there is a marked increase in the number of events below low thresholds, indicating that calmer conditions are projected to occur during this season. An analysis of the simulated wind directions indicates that, during winter, the frequency of north-westerly winds will increase by up to 7% and south-westerly flows will decrease by a similar amount over Switzerland. These results

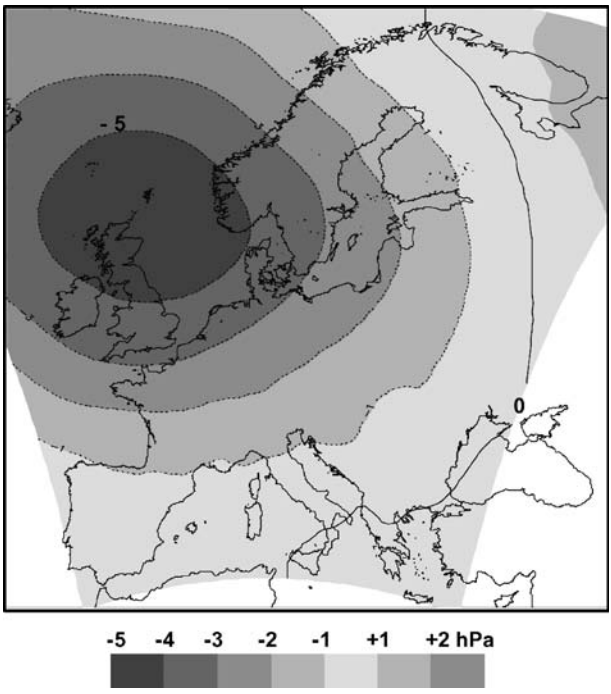

Fig. 9 Simulation by the CHRM regional climate model of the change (hPa) in the winter (DJF) mean of the mean sea level pressure in Europe, between the 1961–1990 and the 2071–2100 periods. Positive change is drawn in *dotted line*

agree with Stefanicki et al. (1998) and Schiesser et al. (1997). Such conditions could lead to an enhanced occurrence of extreme windstorms such as the February 1990 *Vivian* storm or the December 1999 *Lothar* storm.

4.3.2 Modeling of North Sea storm surge climate

Over the last century, floods have had a severe impact on the coastlines of the North Sea, where they can threaten human life as well as property. For a given stretch of coastline, the extent of a storm flood depends directly on wind speed and wind direction. When winds push water towards the coast, it tends to accumulate in a *storm surge*. Serious flooding usually results when a high surge occurs together with a tidal maximum. Flather et al. (1998) and Kauker and Langenberg (2000), among others, have shown that the long-term statistics of storm surges can be modeled satisfactorily with hydrodynamic models. Barotropic models, which operate with vertically integrated state variables, are sufficient for modeling water level variations around the North Sea (Kauker and Langenberg 2000).

Such models can be used not only to reconstruct the history of water-level variations but also to estimate possible future storm surge statistics (Flather and Smith 1998; Langenberg et al. 1999; Lowe et al. 2001; Kaas et al. 2001). Scenarios are obtained by running the hydrodynamic model twice: first with wind and pressure conditions simulated by a high-resolution RCM under 'control' conditions (i.e. with present day atmospheric greenhouse gas loadings) and then under enhanced greenhouse gas concentrations. In the WASA project (Langenberg et al. 1999; Flather and Smith 1998) the wind and pressure data were obtained from two 5-year simulations, in comparison to the 30-year time slices that were used in the STOWASUS project (Kaas et al. 2001). A barotropic hydrodynamic model has

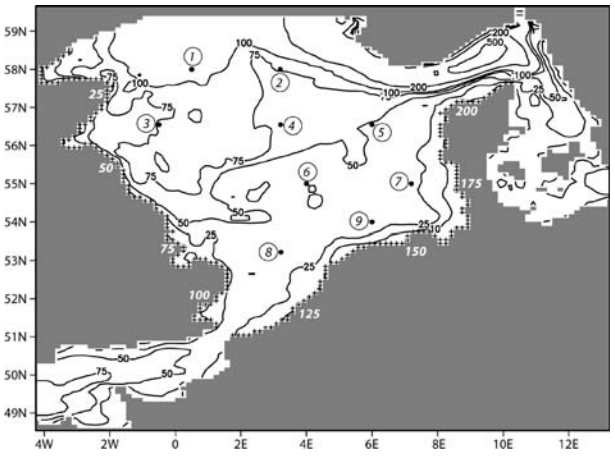

Fig. 10 TRIM integration area, the bathymetry (*isolines*) and the 209 near-coastal grid cells (*crosses*) located along the North Sea coast. *The numbered locations* indicate the selected grid cells for the 'storm count' (see Table 3)

also been used in PRUDENCE to conduct paired control and climate-change simulations, but differs from previous studies by dynamically downscaling the regional wind and pressure conditions. This enables changes in storm surge statistics to be assessed using two of the RCM simulations: HIRHAM-H and RCAO-H.

The hydrodynamic model used in the following analysis is the barotropic storm surge model TRIMGEO (Tidal Residual and Intertidal Mudflat model) developed by Casulli and Catani (1994). The model domain covers the North Sea (Fig. 10) with a grid resolution of $6' \times 10'$ in latitude and longitude, corresponding to a grid box size of about 10×10 km. The integration time step is 10 min and the meteorological forcing is prescribed at the surface as a linear interpolation of 6-hourly instantaneous values. At the open boundaries, in the English Channel and along a line between Wick (UK) and Karmøy (Norway), the sea level is prescribed by amplitudes and phases of 17 partial tides.

Woth et al. (2005) and Aspelien and Weisse (2005) have described the model set up for the North Sea region in more detail and demonstrated the capability of the tide-surge model TRIMGEO to realistically describe surge levels for the North Sea. For this purpose, the TRIMGEO model was driven for the last decades with atmospheric hind-cast simulations performed with the 50 km-grid regional model SN-REMO (SN = spectral nudging; REMO, see Jacob et al. 1995), forced by NCEP/NCAR large-scale re-analyses (Feser et al. 2001). In Woth et al. (2005), a time series of the annual winter 99th percentile surge (DJF) for Cuxhaven was derived and compared with the model hind-cast and observations. A correlation coefficient of 0.93 and a root mean square error of 19 cm were found. The relatively large root mean square error is mainly the result of an underestimation by the model simulation of the very stormy winter 1975/76.

4.3.3 Changes in surge-related storminess

The RCAO-H simulation shows an increase in wind velocity under assumed future conditions of up to 1.5 m/s over large areas while the HIRHAM-H simulation reaches an increase up to 2 m/s, which corresponds to an almost 10% increase in wind speeds compared to today.

Table 3 summarizes the changes in the frequency of severe storms. The number of storms is determined by the frequency with which wind thresholds of 17.2 m/s (Beaufort 8; "gale"), 20.8 m/s (Beaufort 9) or 24.5 m/s (Beaufort 10; "storm") are exceeded (Weisse

Table 3 Numbers of Beaufort (Bf.) 8, 9 and 10 storms in nine 50×50 km^2 grid boxes (marked on Fig. 10) in 30-year control (CTL) runs of the HIRHAM-H and RCAO-H models, and differences with a hindcast (HC) and scenario (A2) runs

		1	2	3	4	5	6	7	8	9
HIRHAM										
Bf. 8	CTL	196	201	124	140	128	109	90	83	75
	HC-CTL	28	42	59	79	78	55	59	53	49
	A2-CTL	−5	11	8	22	19	31	22	32	19
Bf. 9	CTL	25	31	15	16	11	11	11	8	8
	HC-CTL	62	43	44	35	31	39	17	27	28
	A2-CTL	18	13	10	14	15	10	4	10	10
Bf. 10	CTL	3	3	0	0	0	0	0	0	0
	HC-CTL	16	8	7	10	8	8	4	7	4
	A2-CTL	3	7	4	3	1	2	4	1	1
RCAO										
Bf. 8	CTL	202	195	141	161	127	122	90	121	67
	HC-CTL	22	48	42	58	79	42	59	15	57
	A2-CTL	7	4	47	38	36	71	45	48	31
Bf. 9	CTL	29	31	15	15	11	10	6	9	4
	HC-CTL	58	43	44	36	31	40	22	26	32
	A2-CTL	15	17	6	6	9	8	5	9	6
Bf. 10	CTL	2	4	0	0	0	0	0	0	0
	HC-CTL	17	7	7	10	8	8	4	7	4
	A2-CTL	2	−1	2	1	1	1	2	0	1

et al. 2005) during winter (DJF). Results are presented for the hindcasts (1961–90; Feser et al. 2001) and for both the control and A2-scenario runs of HIRHAM-H and RCAO-H in nine selected grid boxes (for the numbering of locations, refer to Fig. 10). The control simulations of both RCMs generate markedly fewer gale and storm events than the hindcast experiment. For gales, the ratio between the number of simulated and hindcast events varies between 33 and 85%, for storms between 60 and 70%. Very strong storms (>32.7 m/s or Beaufort 12) are formed, albeit rarely, in the hindcast, but never in the control or scenario simulations. The number of moderate storms (Beaufort 8) increases by up to 55% from the control to the A2 scenario in most of the nine grid boxes with RCAO-H, but by only up to 30% with HIRHAM-H. In contrast, the number of strong storms (Beaufort 9) doubles in HIRHAM-H but only increases by 50% in RCAO-H. Thus both RCMs show an underestimation of strong wind speeds over this area. This certainly leads to an underestimation of strong surge events (Woth et al. 2005; Flather and Smith 1998). As a result of the deviations between hindcast and control simulations, we interpret the differences between scenario and control climate projections as a relative shift of present day statistics in the projected future. By doing so, we assume that the systematic errors in both the control and the scenario simulations remains the same. This assumption is inherent in all climate change studies and represents the best possible option to date.

4.3.4 Changes in North Sea coastal storm surge statistics

Storm surges, defined as the water level minus the astronomical tide, emerges from the interplay of local wind and air pressure, the characteristics of the coastline and the

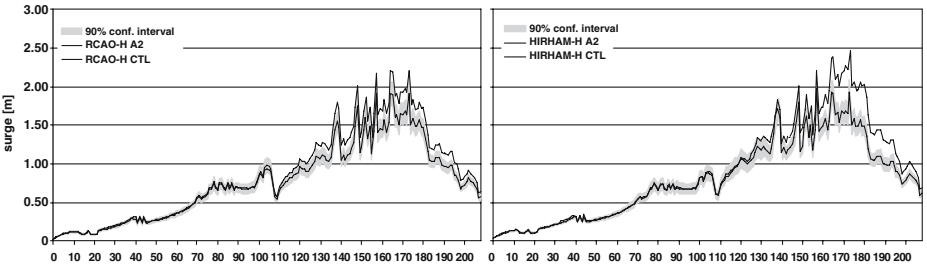

Fig. 11 Mean of winter maximum surge levels in meters from the 30-year control simulation (*black line*) and A2 SRES scenario (*grey line*) for 209 near-coastal locations along the North Sea coast (indicated as crosses in Fig. 10). *Left*: HIRHAM model, *right*: RCAO model. *Shaded area*: 90% confidence interval for present natural variability

bathymetry. To separate the surge from the full sea level variations, a tide-only model run was performed without any meteorological forcing and the resulting water heights were subtracted from the climate response simulations. The effect of the expected rise in mean sea level due to the changing volume of the global ocean is not taken into account. Storm surge residuals were analyzed for 209 grid cells selected along the North Sea coast, extending from Wick (UK) to Skagen (Denmark; see Fig. 10).

Figure 11 compares the modeled surge forced with RCAO-H and HIRHAM-H data for present-day conditions and for the A2 scenario. The maximum of the modeled surge for each year was selected and averaged across each of the two 30-year periods. The grey shaded band marks the 90% confidence intervals based on Student's *t* distribution, reflecting the inter-annual variability (von Storch and Zwiers 1999). Scenario averages falling outside this band indicate significant changes. Along the UK coast, no significant change occurs. Along the Dutch, German and Danish coasts, however, the curve is above the grey band, suggesting an increase in the mean maximum winter surge for the A2 scenario. The increase reaches 50 cm for the HIRHAM-H forcing but only 25 cm for RCAO-H. However both control runs underestimate the amplitude of the mean maximum surge found in the hindcast (not shown). This bias occurs as a consequence of the underestimation of high wind speeds in the atmospheric forcing as discussed by Flather and Smith (1998). However the difference between the HIRHAM-H and RCAO-H simulations is consistent with the analyzed change in high wind speed mentioned earlier. The findings suggest that under future climate conditions, storm surge extremes may increase along the North Sea coast towards the end of this century. In addition, the expected increase in mean sea level for the same time horizon, could lead to an additional 40 cm increase of water level elevations (IPCC 2001), which should be taken into consideration when discussing future security standards and levels for coastal protection.

In summary, both the intensity of westerly wind speed extremes and the number of North Sea gales increase in both RCM simulations. Thus an increase of storm surge elevations is likely under these assumptions. Detailed analysis of future changes in near-surface wind speed extremes over Europe and differences due to RCMs used in the PRUDENCE project can be found in Rockel and Woth (2007). More comprehensive studies concerning changes in North Sea storm surge statistics under climatic change conditions were published in Woth et al. (2005) and in Woth (2005) where a series of driving GCMs, RCMs and different emission scenarios were considered. This made it

possible to investigate the evolution of storm surges also taking into account the uncertainty inherent in these studies.

5 Conclusions

Because of their large impacts on Europe, this paper has focused on heat waves, heavy precipitation events, drought, winter storms, and resulting sea surges. A variety of diagnostic methods were applied to determine how these events are predicted to change by the end of the twenty first century in the set of PRUDENCE RCM experiments. A summary of the main results follows.

- Heat waves – Regional surface warming causes the frequency, intensity and duration of heat waves to increase over Europe. By the end of the twenty first century, countries in central Europe will experience the same number of hot days as are currently experienced in southern Europe. The intensity of extreme temperatures increases more rapidly than the intensity of more moderate temperatures over the continental interior due to increases in temperature variability. These findings are consistent across the global and regional models considered here.
- Precipitation – Heavy winter precipitation increases in central and northern Europe and decreases in the south; heavy summer precipitation increases in north-eastern Europe and decreases in the south. These changes, which are weaker for the B2 than for the A2 scenario, are more robust to RCM in winter than in summer and reflect changes in mean precipitation. However, model choices can have greater effects on the magnitude (RCM) and pattern (GCM) of response than the choice of scenario. The RCMs all predict earlier and longer droughts in the Mediterranean.
- Winter storms – Extreme wind speeds increase between 45° and 55°N, except over and south of the Alps, and become more north-westerly, but the magnitude of the increase depends on RCM. These changes are associated with reductions in mean sea-level pressure and generate more North Sea storms, leading to increases in storm surges along the North Sea coast, especially in Holland, Germany and Denmark.

The use of a consistent set of boundary conditions for all regional climate models, as it was used in the PRUDENCE project, was an opportunity to study the role of RCM formulation to scenario uncertainty. In this respect we find the strongest sensitivity for heavy precipitation in summer. Despite similar GCM forcing, RCMs arrive at changes for precipitation extremes that vary considerably in magnitude and sign. This implies that RCM formulation contributes to scenario uncertainty and that it is not a waste of resources if multi-model ensemble systems, devoted to estimating scenario uncertainties, include a set of RCMs nested into the same GCM, alongside the nesting of RCMs in several different GCMs. This is further substantiated in Frei et al. (2005).

This paper has presented highlights from the most comprehensive regional climate change study performed for Europe. Many intriguing and pressing issues have emerged and many more studies now need to be performed to investigate in more detail the initial findings presented here. Perhaps one of the major weaknesses of this project is that boundary conditions have been provided by only two GCMs, so that the full spectrum of possible transient scenarios has not been entirely sampled. This could affect both the patterns and magnitudes of responses, while RCMs have been found to affect mainly magnitudes. Although RCM simulations provide useful spatial detail for impacts studies,

considerable uncertainties therefore remain about the responses of some extreme events to changes in atmospheric composition.

Despite the uncertainties present in these model simulations of future climate, it is clear that the regional changes in extremes presented here will cause Europe to face some major societal challenges in forthcoming decades.

Acknowledgements The majority of this work has been funded by the European Union Framework 5 project PRUDENCE (EVK2-CT-2100-00132). The Swiss partners of PRUDENCE received funding from the Swiss Ministry for Education and Research. ETH also received funding from the EU project STARDEX (EVK2-CT-2001-00115). We wish to thank other participants of the PRUDENCE project for their invaluable comments on this work. NCEP/NCAR data provided by the NOAA-CIRES Climate Diagnostics Center, Boulder, Colorado, from their Web site at http://www.cdc.noaa.gov/

References

Aspelien T, Weisse R (2005) Assimilation of sea level heights into a regional ocean model for the north sea. Submitted to Ocean Dynamics doi:10.1007/s10236-005-0041-2 (in press)

Beniston M (2003) Climatic change in mountain regions: a review of possible impacts. Clim Change 59:5–31

Beniston M (2004) The 2003 heat wave in Europe: a shape of things to come? Geophys Res Lett 31:L02202

Beniston M, Jungo P (2002) Shifts in the distributions of pressure, temperature and moisture in the alpine region in response to the behavior of the North Atlantic oscillation. Theor Appl Climatol 71:29–42

Beniston M, Stephenson DB (2004) Extreme climatic events and their evolution under changing climatic conditions. Glob Planet Change 44:1–9

Casulli V, Cattani E (1994) Stability, accuracy and efficiency of a semi-implicit method for three-dimensional shallow water flow. Comput Math Appl 27:99–112

Chang EKM, Fu YF (2002) Interdecadal variations in Northern Hemisphere winter storm track intensity. J Climate 15(6):642–658

Christensen JH, Christensen OB (2003) Severe summertime flooding in Europe. Nature 421:805–806

Christensen JH, Carter TR, Giorgi F (2002) PRUDENCE employs new methods to assess European climate change. EOS 83:13

Christensen OB, Christensen JH, Machenhauer B, Botzet M (1998) Very high-resolution regional climate simulations over Scandinavia-present climate. J Clim 11:3204–3229

Coles S (2001) An introduction to statistical modeling of extreme values. Spinger, Berlin Heidelberg New York

Ferro CAT, Hannachi A, Stephenson DB (2005) Simple non-parametric techniques for exploring changing probability distributions of weather. Submitted to J Climate (in press)

Feser F, Weisse R, von Storch H (2001) Multidecadal atmospheric modelling for Europe yields multi-purpose data. EOS 82:305+310

Fischer PH, Brunekreef B, Lebret E (2004) Air pollution related deaths during the 2003 heat wave in The Netherlands. Atmos Environ 38:1083–1085

Flather R, Smith J (1998) First estimates of changes in extreme storm surge elevations due to doubling CO2. Global Atmos Ocean Syst 6:193–208

Flather R, Smith J, Richards J, Bell C, Blackman D (1998) Direct estimates of extreme surge elevations from a 40 year numerical model simulation and from observation. Global Atmos Ocean Syst 6:165–176

Frei C (2003) Statistical limitation for diagnosing changes in extremes from climate model simulations. Proc. 14th Sympos. on global change and climate variations. AMS Annual Meeting 2003, Long Beach, CA. On CD-ROM, p 6

Frei C, Schär C (2001) Detection probability of trends in rare events: theory and application to heavy precipitation in the Alpine region. J Climate 14:1564–1584

Frei C, Schöll R, Schmidli J, Fukutome S, Vidale PL (2005) Future change of precipitation extremes in Europe: an intercomparison of scenarios from regional climate models. J Geophys Res 110(D3):4124–4137

Frich P, Alexander LV, Della-Marta P, Gleason B, Haylock M, Klein Tank AMG, Peterson T (2002) Observed coherent changes in climatic extremes during the second half of the twentieth century. Clim Res 19:193–212

Goyette S, Brasseur O, Beniston M (2003) Application of a new wind gust parameterisation; multi-scale case studies performed with the Canadian RCM. J Geophys Res 108:4371–4389

Harnik N, Chang EKM (2003) Storm track variations as seen in radiosonde observations and reanalysis data. J Climate 16:480–495
Huth R, Kysely J, Pokorna I (2000) A GCM simulation of heat waves, dry spells, and their relationships to circulation. Clim Change 46:29–60
IPCC (2001) Climate change 2001: the scientific basis. Cambridge University Press, Cambridge, UK, p 881
Jacob D (2001) A note to the simulation of the annual and interannual variability of the water budget over the Baltic Sea drainage basin. Meteorol Atmos Phys 77:61–73
Jacob D, Podzun R, Claussen M (1995) REMO-A model for climate research and weather prediction. International workshop on limited-area and variable resolution models, Beijing, China, October 23–27, 1995, pp 273–278
Jacob D et al (2007) An intercomparison of regional climate models for Europe: design of the experiments and model performance. Clim Change, doi:10.1007/s10584-006-9213-4 (this issue)
Johns TC et al (2003) Anthropogenic climate change for 1860 to 2100 simulated with the HadCM3 model under updated emission scenarios. Clim Dyn 20:583–612
Jones R, Murphy J, Hassell D, Taylor R (2001) Ensemble mean changes in a simulation of the European climate of 2071–2100, using the new Hadley Centre regional climate modelling system HadAM3H/HadRM3H. Hadley Centre Report 2001, available from http://prudence.dmi.dk
Kaas E, Andersen U, Flather RA, Willimas JA, Blackman DL, Lionello P, Dalan F, Elvini E, Nizzero A, Malguzzi P, Pfizenmayer A, von Storch H, Dillingh D, Phillipart M, de Ronde J, Reistad M, Midtbø KH, Vignes O, Haakenstad H, Hackett B, Fossum I, Sidselrud L (2001) Synthesis of the STOWASUS-2100 project: regional storm, wave and surge scenarios for the 2100 century. Danish Climate Centre Report 01–3:22
Katz RW, Brown BG (1992) Extreme events in a changing climate: variability is more important than averages. Clim Change 21:289–302
Kauker F, Langenberg H (2000) Two models for the climate change related development of sea levels in the North Sea. A comparison. Clim Res 15:61–67
Kharin VV, Zwiers FW (2000) Changes in the extremes in an ensemble of transient climate simulations with a coupled atmosphere-ocean GCM. J Climate 13:3760–3788
Kundzewicz ZW, Szamalek K, Kowalczak P (1999) The great flood of 1997 in Poland. Hydrol Sci J 44:855–870
Langenberg H, Pfizenmayer A, von Storch H, Sündermann J (1999) Storm related sea level variations along the North Sea coast: natural variability and anthropogenic change. Cont Shelf Res 19:821–842
Lenderink G, van den Hurk B, van Meijgaard E, van Ulden A, Cuipers H (2003) Simulations of present-day climate in RACMO2: first results and model development. Royal Netherlands Meteorological Institute Technical Report, De Bilt, The Netherlands
Lowe JA, Gregory JM, Flather RA (2001) Changes in the occurrence of storm surges around the United Kingdom under a future climate scenario using a dynamic storm surge model driven by the Hadley Centre climate models. Clim Dyn 18:179–188
Lüthi D, Cress A, Davies HC, Frei C, Schär C (1996) Interannual variability and regional climate simulations. Theor Appl Climatol 53:185–209
McGregor GR, Ferro CAT, Stephenson DB (2005) Projected changes in extreme weather and climate events in Europe. In: Kirch W, Menne B, Bertollini R (eds) Extreme weather and climate events and public health responses vol. 13–23 Dresden. Springer, Berlin Heidelberg New York, p 303
Mearns LO, Katz RW, Schneider SH (1984) Extreme high-temperature events: changes in their probabilities with changes in mean temperature. J Clim Appl Meteorol 23:1601–1613
Meehl GA, Zwiers F, Evans J, Knutson T, Mearns L, Whetton P (2000) Trends in extreme weather and climate events: issues related to modelling extremes in projections of future climate change. Bull Am Meteorol Soc 81:427–436
Munich Re (2002) Topics, an annual review of natural catastrophes. Munich Reinsurance Company Publications, Munich, 49 pp
Nakićenović N et al (2000) IPCC special report on emissions scenarios, Cambridge University Press, Cambridge, UK, p 599
Otterman J, Angell JK, Ardizzone J, Atlas R, Schubert S, Starr D, Wu ML (2002) North-Atlantic surface winds examined as the source of winter warming in Europe. Geophys Res Lett 29, art. no. 1912
Pope DV, Gallani M, Rowntree R, Stratton RA (2000) The impact of new physical parameterizations in the Hadley Centre climate model HadAM3. Clim Dyn 16:123–146
Räisänen J, Hansson U, Ullerstig A, Döscher R, Graham LP, Jones C, Meier M, Samuelsson P, Willén U (2004) European climate in the late 21st century: regional simulations with two driving global models and two forcing scenarios. Clim Dyn 22(1):13–31
Robinson PJ (2001) On the definition of a heat wave. J Appl Meteorol 40:762–775

Rockel B, Woth K (2007) Future changes in near surface wind speed extremes over Europe from an ensemble of RCM simulations. Clim Change, doi:10.1007/s10584-006-9227-y (this issue)
Roeckner E et al (2003) The atmospheric general circulation model ECHAM 5. PART I: model description, MPI-Report 349, Hamburg, Germany
Schär C, Vidale PL, Lüthi D, Frei C, Häberli C, Liniger M, Appenzeller C (2004) The role of increasing temperature variability in European summer heatwaves. Nature 427:332–336
Schiesser HH, Pfister C, Bader J (1997) Winter storms in Switzerland North of the Alps 1864/65–1993/94. Theor Appl Climatol 58:1–19
Shabbar A, Bonsal B (2003) An assessment of changes in winter cold and warm spells over Canada. Nat Hazards 29:173–188
Siegismund F, Schrum C (2001) Decadal changes in the wind forcing over the North Sea. Climate Res 18:39–45
Stedman JR (2004) The predicted number of air pollution related deaths in the UK during the August 2003 heatwave. Atmos Environ 38:1087–1090
Stefanicki G, Talkner P, Weber RO (1998) Frequency changes of weather types in the Alpine region since 1945. Theor Appl Climatol 60:47–61
Steppler J, Doms G, Schättler U, Bitzer HW, Gassmann A, Damrath U, Gregoric G (2003) Meso-gamma scale forecasts using the nonhydrostatic model LM. Meteorol Atmos Phys 82:75–96
Swiss Re (2003) Natural catastrophes and reinsurance. Swiss Reinsurance Company Publications, Zürich, p 47
Ulbrich U, Christoph M (1999) A shift of the NAO and increasing storm track activity over Europe due to anthropogenic greenhouse gas forcing. Clim Dyn 15:551–559
Ulbrich U, Fink AH, Klawa M, Pinto JG (2000) Three extreme storms over Europe in December 1999. Weather 56
von Storch H, Zwiers FW (1999) Statistical analysis in climate research. Cambridge University Press, Cambridge, UK, ISBN 0 521 45071 3, p 494
Weisse R, von Storch H, Feser F (2005) Northeast Atlantic and North Sea storminess as simulated by a regional climate model 1958–2001 and comparison with observations. J Climate 18(3):465–479
Woth K (2005) North sea storm surge statistics based on projections in a warmer climate: how important are the driving GCM and the chosen emission scenario? Geophysical Res Lett 32:L22708, doi:10.1029/2005GL02372
Woth K, Weisse R, von Storch H (2005). Climate change and North Sea storm surge extremes: an ensemble study of storm surge extremes expected in a changed climate projected by four different Regional Climate Models. Ocean Dyn 56(1):3–15, doi:10.1007/s10236-005-0024-3 (in press)
Zwiers FW, Kharin VV (1998) Changes in the extremes of the climate simulated by CCC GCM2 under CO_2 doubling. J Climate 11:2200–2222